ELSEVIER

Biophysical Chemistry 82 (1999) 9–22

Biophysical Chemistry

www.elsevier.nl/locate/bpc

A molecular dynamics simulation study of the solvent isotope effect on copper plastocyanin

Rita Guzzi[a,*], Caterina Arcangeli[b], Anna Rita Bizzarri[b]

[a] *Unita' INFM, Dipartimento di Fisica, Universita' della Calabria, I-87030 Rende, Italy*
[b] *Unita' INFM, Dipartimento di Scienze Ambientali, Universita' della Tuscia, I-01100 Viterbo, Italy*

Received 5 March 1999; received in revised form 29 July 1999; accepted 29 July 1999

Abstract

The effect of heavy water on the structure and dynamics of copper plastocyanin as well as on some aspects of the solvent dynamics at the protein–solvent interfacial region have been investigated by molecular dynamics simulation. The simulated system has been analyzed in terms of the atomic root mean square deviation and fluctuations, intraprotein H-bond pattern, dynamical cross-correlation map and the results have been compared with those previously obtained for plastocyanin in H_2O (Ciocchetti et al. Biophys. Chem. 69 (1997), 185–198). The simulated plastocyanin structure in the two solvents, averaging 1 ns, is very similar along the β-structure regions, while the most significant differences are registered, analogous to the turns and the regions likely involved in the electron transfer pathway. Moreover, plastocyanin in D_2O shows an increase in the number of both the intraprotein H-bonds and the residues involved in correlated motions. An analysis of the protein–solvent coupling evidenced that D_2O makes the H-bond formation more difficult with the solvent molecules for positively charged and polar residues, while an opposite trend is observed for negatively charged residues. On the other hand, the frequency of exchange of the solvent molecules involved in the protein–solvent H-bond formation is significantly depressed in D_2O. The results are discussed also in connection with protein functionality and briefly with some experimental results connected with the thermostability of proteins in D_2O.

Keywords: Plastocyanin; Solvent isotope; Molecular dynamics

* Corresponding author. Fax: +39-984-493187.
E-mail address: guzzi@fis.unical.it (R. Guzzi)

0301-4622/99/$ - see front matter
PII: S0301-4622(99)00097-6

1. Introduction

To perform their biological function, most proteins fold to globular conformations that are stabilized by many different non-covalent interactions. Among these, the protein–solvent interaction, which reflects the mutual influence of both water and protein on each other, plays a very important role [1]. Water molecules exert their action through the H-bond network in maintaining the proper tertiary structure of the protein and participating in structural fluctuations. Indeed, protein dehydration gives rise to conformational changes which can induce the inactivation of the biological functionality [2,3]. On the other hand, the properties of the solvent are also strongly influenced by the presence of the protein. In fact, the protein surface is able to modulate the water mobility and then to cause an anomalous behavior of the water molecules at distances close enough to the protein surface [4–7].

Insight into the role of solvents can be obtained by studying the effects induced by solvent perturbation on the structure and dynamics of proteins [8–10]. Such a perturbation is usually obtained by adding an organic solvent to the protein solution. However, in order to avoid strong solvent effects on proteins the use of mild perturbative agents is preferable. Since biological macromolecules operate in aqueous solution, the mildest perturbant for light water (H_2O) is its isotopic form, D_2O. Although D_2O and H_2O can essentially be viewed as forming the same liquid, differences in some physical parameters do exist. In particular, higher viscosity, melting point and heat capacity of D_2O with respect to H_2O indicate a higher structural order in heavy water [11,12]. Moreover, because of the different nuclear spin, deuterium oxide is often considered a more suitable solvent with respect to H_2O in NMR studies of biological macromolecules. Similarly, H_2O/D_2O scattering differences can be applied in a powerful way in neutron scattering solvent difference maps [13–15]. Independently of the experimental approach used, the common assumption is that both structure and dynamics of protein as well as the solvent behavior at the interface is similar in H_2O and D_2O.

Recent experimental studies, performed on some small globular proteins [16,10], have shown that D_2O affects the thermodynamics of protein unfolding in a complex way. In fact, the thermostability of proteins (namely the transition temperature between the folded and unfolded state) increases by several degrees. On the other hand, both the enthalpy and entropy of unfolding are significantly reduced in D_2O. Consequently, the resulting Gibbs free energy of unfolding, which defines the stability of a protein, is higher in H_2O than in D_2O. The isotopic substitution of hydrogen by deuterium can affect the strength of the: (i) solvent–solvent; (ii) solute–solute; and (iii) solute–solvent hydrogen bonds [17]. Comparative studies performed on hydrogenated and deuterated proteins suggest that the solvent isotope effect could arise from an increased strength of the solvent–solvent hydrogen bonds in D_2O [12,17]. In other words, it can be hypothesized that the reduced stability of protein in D_2O could result by changes in the protein–solvent coupling induced by a different three-dimensional distribution of the solvent molecules at the interfacial region.

Molecular dynamics (MD) simulation which is, in principle, able to reveal at atomic resolution the details of the structure and dynamics of both protein and solvent atoms, can be considered a useful tool to investigate the protein behavior in different solvents.

So far, the wealth of MD simulation studies on proteins in solution has been performed in H_2O [18–21]. More recently, an accurate parametrization of other solvents has allowed to extend MD simulation to protein dissolved in different solvents [22,23].

In this paper we present a long-term (1.1 ns) MD simulation of plastocyanin (PC) in D_2O aimed at investigating the isotopic effect on its structure and dynamics, also paying attention to the structural elements likely involved in the electron transfer pathway. Some aspects concerning the solvent organization at the interfacial region are also discussed. The comparison of these results

with those previously obtained in a MD simulation of PC in H_2O [24] allows us to put demonstrate that both the structure and dynamics of PC as well as the solvent dynamics at the interfacial regions are affected by the isotopic substitution. A possible connection between the observed effects on PC and some experimental properties of the proteins in D_2O is also suggested.

2. Computational methods

The MD simulation of PC fully hydrated in deuterium oxide has been performed using the GROMOS87 program package including the SPC/E potential [25]. The effect of deuteration was modeled by doubling the mass of the hydrogen of the 3501 solvent molecules included in the simulation [19].

The initial coordinates of the 885 PC atoms, the copper ion and the 110 crystallization water molecules have been obtained by the X-ray crystal structure at 1.33 Å (1PLC from Protein Data Bank) [26]. The copper ion is located in a hydrophobic region at approximately 6 Å from the protein surface and is coordinated by two S and two N atoms in a distorted tetrahedral array [27]. To describe the copper–ligand interaction, a covalent bond was introduced for each ligand to preserve the X-ray structure [28]. This assumption finds a ground on an experimental basis [27]. The protein molecule was centered in a truncated octahedron obtained from a cube of edge 6.20257 nm. The minimum distance between the solute atoms and the box edge was 1.06 nm. Periodic boundary conditions were applied to avoid edge effects. Cut off radii of 0.8 and 1.4 nm for the non-bonded and long-range interactions were used, respectively.

During the 105 steps of energy minimization with the steepest descent method, anharmonic position restraining with a force constant of 9000 $KJ/mol/nm^2$ was used to minimize the root mean square deviation (RMSD) from the X-ray structure. Initial atomic velocities were assigned from a Maxwellian distribution corresponding to 250 K. Any residual translational and rotational motion of the center of mass was removed from the initial velocities. The temperature was fixed at 250 K during the first 6 ps, then it was increased by 5 K every 4 ps to reach the final value of 300 K, which was maintained throughout the remaining simulation time. The temperatures of both protein and solvent were separately coupled to an external bath with relaxation times of 0.1 ps. The pressure was kept constant by a coupling to a pressure bath at 1.013 bar with a relaxation time of 0.5 ps. A decreasing positional restrained force, with a constant going from 9000 to 50 $KJ/mol/nm^2$ was also applied during the first 40 ps. The MD simulation has been followed for a 1100-ps period, the first 100 ps being for equilibration. Configurations of all trajectories and energies were collected every 0.1 ps with a step of integration of 0.002 ps. The Shake constraint algorithm [29] was used throughout the simulation to fix the internal geometry of the water molecules and to keep bond lengths of proteins rigorously fixed at their equilibrium positions.

Table 1
Selected properties of PC in D_2O calculated from the MD simulated trajectories[a]

Parameter	Mean	S.D.	Min	Max	Drift
R_g (nm)	1.255	0.007	1.236	1.284	3.7×10^{-5}
E_{pot} (MJ/mol)	−173.37	0.43	−174.98	−171.76	0.22
E_{kin} (MJ/mol)	28.87	0.20	28.04	29.88	−0.01
RMSD of all atoms (nm)	0.171	0.014	0.150	0.185	1.2×10^{-5}
RMSD of C_α atoms (nm)	0.125	0.012	0.102	0.139	4×10^{-6}

[a]All values are calculated during the 100–1100-ps time interval. S.D.: standard deviation; Min: minimal value; Max: maximal value; RMSD: root mean square deviations; R_g: radius of gyration; E_{pot}: total potential energy; E_{kin}: total kinetic energy. The drift values are calculated from a linear regression and are given per picosecond.

To check for a proper equilibration and convergence of the simulated system, the various components of the energy and the all atom RMSD from the X-ray structure have been calculated as a function of time. The values of some relevant parameters calculated by the MD trajectories are presented in Table 1. The stability of the kinetic and potential energy of the PC–D_2O system is reached after approximately 50 ps, whereas the all atom RMSD show a significant deviation from the crystal structure of PC during the first 100 ps and a small fluctuation of the RMSD around the mean value of 0.171 nm (Table 1) along the remaining simulation time. A smaller value of RMSD is obtained when the analysis is restricted to the C_α atoms (Table 1), in agreement with other protein simulations [30,31]. For the analysis of the structural and dynamical properties of both PC and solvent atoms, the 100–1100 ps data have been taken into account.

For the intraprotein H-bond analysis, the following definitions were used: an H-bond was assumed to occur when the distance between the hydrogen and the acceptor was shorter than 0.32 nm and the donor–acceptor angle was larger than 120°. The frequency of intraprotein H-bonds has been computed and compared with data obtained from crystallography [32]. We have considered as maintained the crystallographic H-bonds which are present during the simulation with a permanence time greater than 25%. Moreover, H-bond interactions between residues have been con-

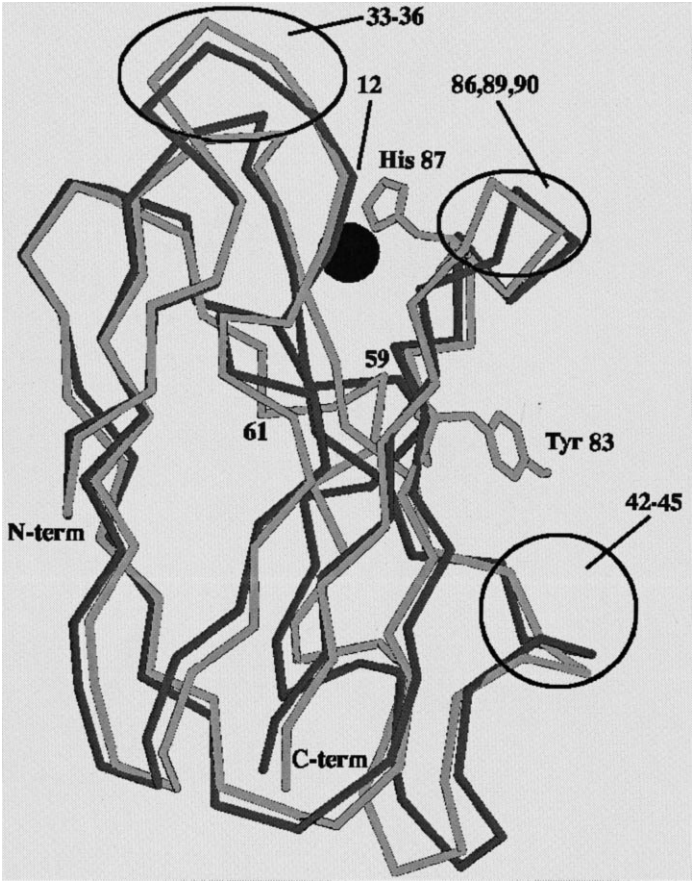

Fig. 1. Snapshots of the main-chain atoms (N, C_α, C and O) of the PC crystal structure (light–grey line) and of the MD simulated structure (dark–grey line) averaged over the 100–1100-ps simulation time. The electron transfer route is also indicated (see the text for the details).

sidered maintained even if the atoms acting as donor or acceptor change in the simulation (for instance the crystallographic H-bond $66N^{\xi}$–$32O^{\delta 1}$, which is replaced by $66N^{\xi}$–$32O$, is considered as conserved in the simulation).

3. Results and discussion

PC belongs to the blue copper protein family and functions as an electron shuttle between cytochrome *f* and photosystem I in plant photosynthetic systems. The protein residues involved in the electron transfer route are grouped and labeled in Fig. 1 [27,33]. The protein regions involved in this route are usually indicated as: hydrophilic patch, which includes residues Asp42–Ser45 and Glu59–Asp61, hydrophobic patch (Leu12, Ala33–Pro36, Gly89–Ala90) and finally Tyr83 and His87. The copper ion is also shown in the upper side of the molecule, (dark sphere). From a structural point of view, PC is formed by eight β-strands, arranged in two β sheets, and from one short region of α-helix. The β-structure is able to mediate distant electronic couplings more efficiently with respect to α-helix; such an efficiency having been related to the H-bonds that are better mediators across the β sheets than through α-helices [34]. Due to its peculiar spectroscopic features, this protein has been the object of intense experimental investigation [35,36]. More recently, in some papers authored by some of us [4,24,28,37], structural and dynamical aspects of the PC–water interaction have been deeply investigated by using an MD simulation approach. From these works an overall picture emerges pointing out a general stiffness of the most important functional regions and a higher mobility of the solvent-exposed regions. Moreover, the investigation of the spatial and temporal organization of water at the protein–solvent interface has evidenced an anomalous diffusional and relaxation behavior of the hydration water [5,37,38].

In this paper, the results of the MD simulation of PC, fully hydrated with D_2O, will be mainly

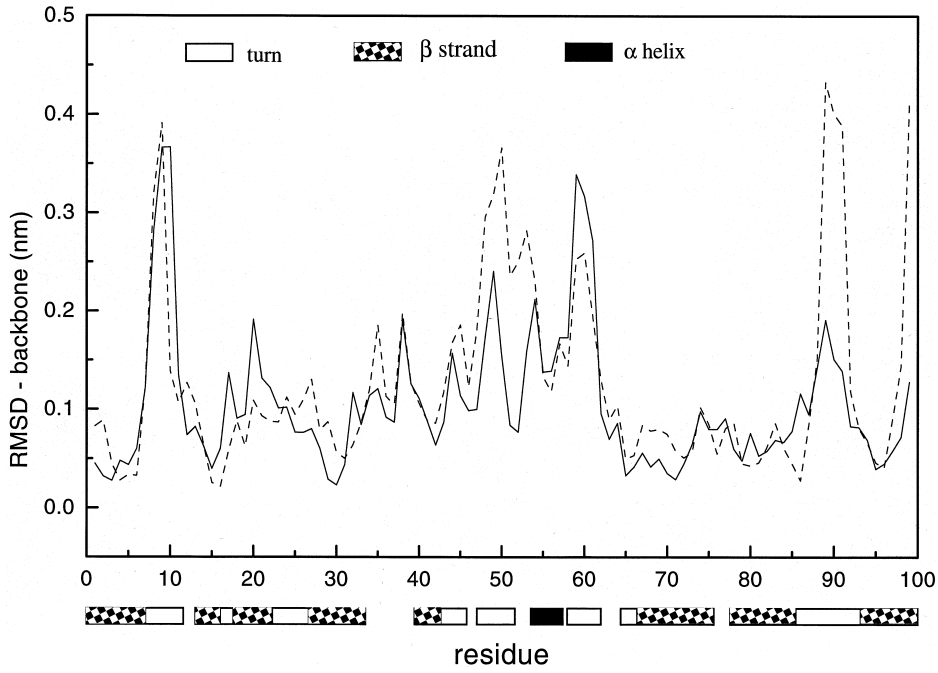

Fig. 2. Time averaged (100–1100 ps) RMSD of the backbone atoms from the X-ray for the simulated structure of PC in D_2O (solid line) and in H_2O (dashed line).

discussed in connection with a previous simulation of PC in H_2O [24], in order to elucidate the solvent isotope effect on the protein structure and dynamics.

Fig. 1 shows a snapshot of the backbone atoms, (N, C_α, C and O), of the PC simulated structure (dark–grey line) averaged over the 100–1100 ps simulation time, superimposed on the crystal structure (light–grey line). As can be seen, the two overall structures are remarkably similar, although some differences can be observed in specific regions.

A comparison of the time averaged RMSD from the X-ray structure, as a function of the residue number of the PC backbone atoms is shown in Fig. 2 for PC in D_2O (solid line) and in H_2O (dashed line). Secondary structure elements are also indicated. The RMSD values obtained in the two solvents are generally small (< 0.2 nm) and are in agreement with other MD simulations [30,31] and are indicative of a close similarity of the two simulated structures with the crystallographic one. In both cases, the regions of the PC structure that mostly deviate from the crystal structure are localized in turns and loops exposed to the solvent. This deviation appears to be almost of the same extent for the peak centered in correspondence of Gly10, while some difference can be observed for the regions Ser45–Ile55, Glu59–Asp61 and Gly89–Gly91. Concerning the functional protein regions, such as the acidic and the hydrophobic patches, it can be observed that, in the presence of D_2O, most of the residues display lower RMSD values, with the exception of the residues Glu59–Asp61 and Pro86.

In order to better characterize the flexibility of the PC atoms, the root mean square fluctuation (RMSF) of atomic positions in the simulation run have been calculated according to:

$$\Delta R = \left(\langle r_i^2 \rangle - \langle r_i \rangle^2\right)^{1/2} = \left[\frac{1}{N_{at}} \sum_{i=1}^{N_{at}} \langle (\Delta x_i)^2 + (\Delta y_i)^2 + (\Delta z_i)^2 \rangle\right]^{1/2} \quad (1)$$

where N_{at} is the total number of atoms, Δx_i, Δy_i and Δz_i are the differences between the instantaneous and averaged atomic coordinates for the i-th atom and the brackets $\langle \ldots \rangle$ indicate a time average. In Fig. 3A, the RMSF values of the backbone atoms of PC in D_2O (solid line) are compared with the corresponding RMSF values derived from the crystallographic B-factors (dotted line). The two plots show that the main peaks are maintained at the same positions while the amplitude of the atomic fluctuations are higher in the presence of D_2O. A similar trend between experimental and simulated B-factors has been reported for BPTI and Lysozyme [31]. The RMSF values of the PC backbone atoms in H_2O, shown in the same figure (dashed–dotted line) for comparison, follow approximately the same behavior of PC in D_2O. For the protein structure in both solvents, the highest RMSF peak is found again in correspondence of Gly10 as in the RMSD plot (Fig. 2). It refers to a solvent-exposed turn which constitutes the most mobile region of the protein. The most significant differences are registered in the region surrounding the α-helix (Glu59–Asp61) and in correspondence of the terminal turn of the protein (Pro86–Ala90), which show higher RMSF values in the D_2O solvent. It is worth remarking that these regions include some of the copper ligands, most of the hydrophobic residues and two residues of the acidic patch which play a crucial role in the electron transfer reaction with the redox partners.

The PC side chain RMSF values in D_2O (Fig. 3B, solid line) are found to be generally higher than those of the backbone atoms. This is similar to what happens in H_2O and is probably due to both the higher flexibility of the lateral chains and the extensive interactions with the solvent, to which these chains are more exposed. On the other hand, a constraint of the backbone atoms is presumably imposed by the rigid arrangement of the β-structure of the protein architecture. A comparison with the RMSF obtained for the side chain atoms in H_2O, (Fig. 3B, dashed line), reveals a close similarity between the two plots. The differences mainly concern the regions Pro16–Ile21, Ser53–Thr69 and Pro86–Lys95. We note that these regions include, as already mentioned,

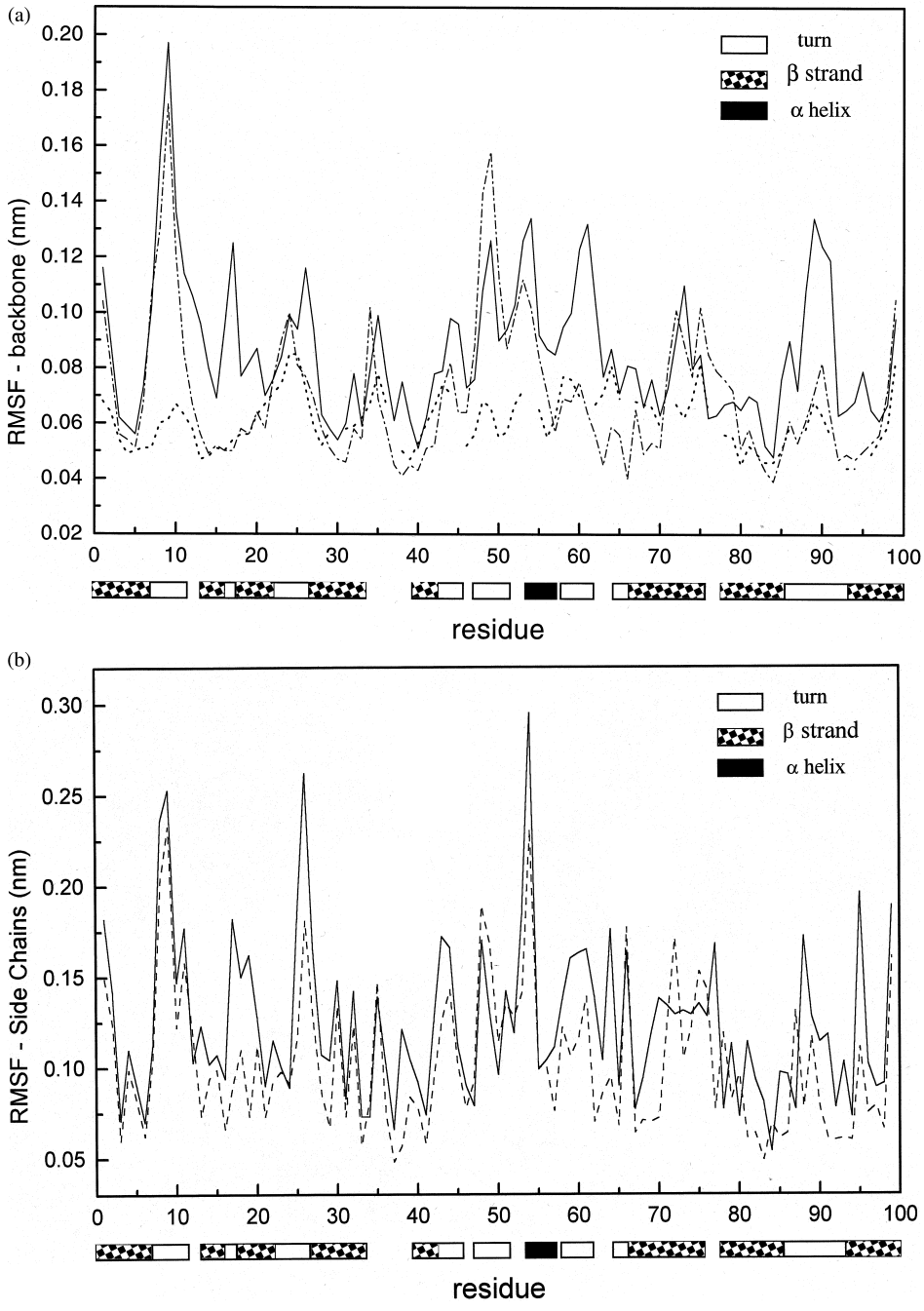

Fig. 3. (a) Comparison between the positional RMSF of the main-chain PC atoms calculated from the simulated structure in D_2O averaged over the (100–1100 ps) simulation time (solid line) and obtained from crystal structure B-factors (dotted line) according to the expression: $(\langle r_i^2 \rangle - \langle r_I \rangle^2) = (3B_i)(8\pi^2)^{-1}$. The RMSF values of the simulated structure in H_2O are also shown (dashed–dotted line). (b) RMSF values of the side-chain atoms of PC in D_2O (solid line) and in H_2O (dashed line).

some of the residues belonging to the protein electron transfer pathway.

In summary, we observe that the protein regions which are likely involved in the electron transfer process, appear more mobile in D_2O than in H_2O. It should be recalled that in the latter solvent the stiffness of these regions and their inaccessibility to solvent were supposed to be important for the functionality of the protein itself [24].

The analysis of the intraprotein H-bond pattern can provide further information on the effect induced by D_2O on the protein structure and dynamics. Before we discuss these set of data it should be pointed out that no H/D exchange between protein and solvent has been taken into account because the exchange time scale is much longer than the simulation time. In fact, 10^{-7} s are required for isotopic exchange of the exposed hydrogens [39] while, much longer time, ranging

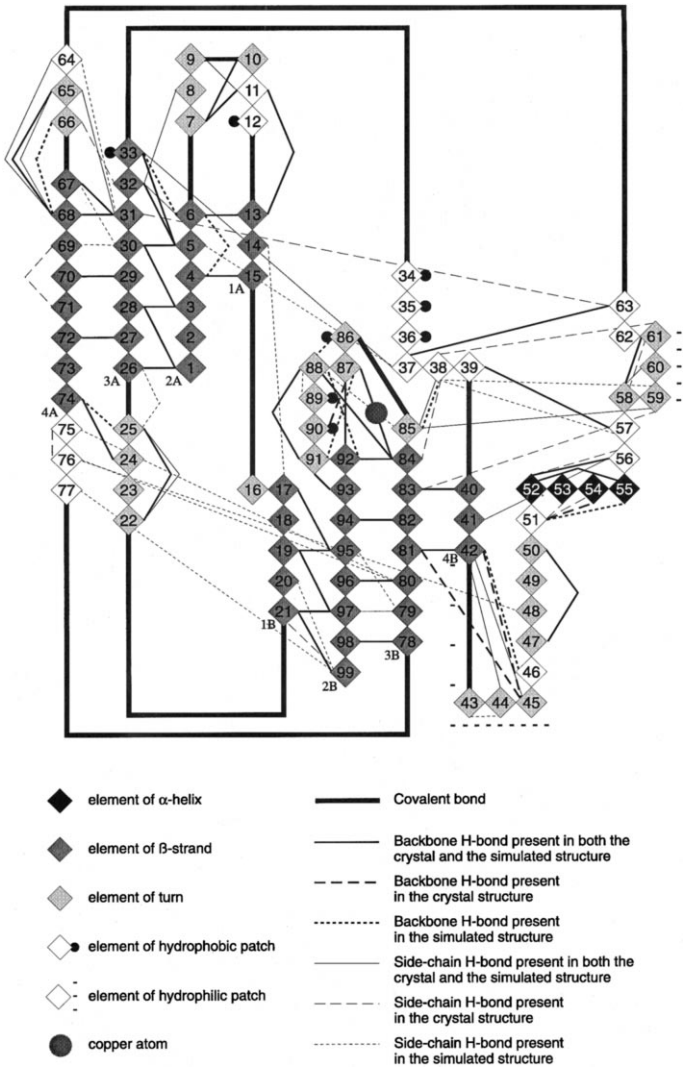

Fig. 4. Diagram of the hydrogen bond patterns for the crystal and the simulated structure of PC in D_2O. The MD derived intraprotein H-bonds shown are only those having a permanence time greater than 25%. Grey intensity represents the secondary structure of residues as defined by crystallographic results. The copper ion, the acidic and hydrophobic patches are also shown.

from second to month, are required for the exchange of amide hydrogens [40].

Fig. 4 shows an overall picture of the intraprotein H-bonds, obtained in the simulation of PC in D_2O compared to the crystallographic hydrogen bond pattern. The data are related to the secondary structure of the protein, the acidic and hydrophobic patches and the copper ion. The MD H-bonds shown in the picture are only those having a permanence time greater than 25% with respect to the simulation time considered for the data analysis (100–1100 ps). With respect to crystallography, it turns out that four backbone and five side-chain H-bonds are lost during the simulation. On the other hand, the formation of new H-bonds, mainly among elements of the secondary structure belonging to different sheets, is observed. The copper site environment is also involved in the rearrangement of the H-bond network. In fact, the Gly91 residue replaces Ala90 in the X-ray backbone H-bond with His87, which is the only copper ligand located on the protein surface. Within the two patches, the hydrophobic one forms six new H-bonds (four among the backbone atoms and two involving the side chains). Only one additional H-bond is found in the hydrophilic patch during the 1000 ps analyzed. The formation of new H-bonds within the functional regions is of some interest for the possible influences on the electron transfer process [41].

The comparison of the intraprotein H-bonds obtained from the MD simulations of PC in H_2O and in D_2O, averaging the trajectory data between 100 and 1100 ps, shows that in the presence of D_2O a higher number of new H-bonds is formed. The complete list of the new H-bonds involving backbone and side-chain atoms is given in Table 2.

The overall increase of the intraprotein H-bonds registered during the 1.1 ns simulation of PC in D_2O could indicate that this solvent induces a modification of the protein conformation, towards a more compact form which is compatible with an approaching of the atoms able to form H-bonds. This packing could be consistent with the higher hydrophobic character of D_2O compared to H_2O which, in turn, could be ascrib-

Table 2
List of the new intramolecular hydrogen bonds involving backbone (Group 1) and side-chain (Group 2) atoms derived from the MD simulation of PC in H_2O and D_2O with respect to the crystallographic data. The atoms involved in the H-bonds are indicated in parentheses

Residue		Permanence time (%)	
Donor	Acceptor	H_2O[a]	D_2O[b]
Group 1			
*Gly*6 (*N*)	*Leu*4 (*O*)	55.5	42.2
*Phe*14 (*N*)	*Gly*91 (*O*)	96.6	5.5
*Ala*33 (*N*)	*Gly*6 (*O*)	–	46.8
*Ile*39 (*N*)	*Met*57 (*O*)	–	29.8
*Ile*46 (*N*)	*Asp*42 (*O*)	98.5	93.2
*Ile*55 (*N*)	*Asp*51 (*O*)	91.6	80.8
*Glu*68 (*N*)	*Lys*66 (*O*)	–	25.3
*Leu*74 (*N*)	*Glu*25 (*O*)	95.1	61.4
*Ser*85 (*N*)	*Asn*38 (*O*)	97.4	86.9
*Gly*91 (*N*)	*His*87 (*O*)	–	68.7
*Met*92 (*N*)	*Gln*88 (*O*)	–	28.5
Group 2			
*Asp*2 (*N*)	*Asp*2 ($O^{\delta 2}$)	–	28.8
*Asp*9 (*N*)	*Asp*9 ($O^{\delta 1}$)	47.3	–
*Ser*11 (O^{γ})	*Asp*9 ($O^{\delta 2}$)	–	49.6
*Ser*17 (O^{γ})	*Phe*14 (*O*)	–	27.2
*Ser*22 (*N*)	*Glu*25 ($O^{\varepsilon 1}$)	42.3	–
*Ser*22 (O^{γ})	*Glu*25 ($O^{\varepsilon 1}$)	53.9	–
*Ser*22 (O^{γ})	*Glu*25 ($O^{\varepsilon 2}$)	77.3	–
*Lys*26 (*N*)	*Glu*25 ($O^{\varepsilon 2}$)	–	26.9
*Lys*30 (N^{η})	*Glu*67 (*O*)	–	28.4
*Lys*30 (N^{η})	*Thr*69 ($O^{\gamma 1}$)	–	33.8
*Asn*31 ($N^{\delta 2}$)	*Asn*64 (*O*)	50.2	45.6
*Asn*32 ($N^{\delta 2}$)	*Asp*8 ($O^{\delta 2}$)	–	27.2
*His*37 ($N^{\varepsilon 2}$)	*Leu*5 (*O*)	–	33.8
*Asn*38 ($N^{\delta 2}$)	*Met*57 (*O*)	92.0	54.6
*Asn*38 ($N^{\delta 2}$)	*Glu*59 ($O^{\varepsilon 2}$)	83.8	51.6
*Glu*43 (*N*)	*Glu*43 ($O^{\varepsilon 1}$)	–	35.6
*Asp*44 (*N*)	*Glu*43 ($O^{\varepsilon 2}$)	–	49.6
*Ser*45 (*N*)	*Asp*42 ($O^{\delta 1}$)	68.6	25.1
*Ser*45 (O^{γ})	*Asp*42 ($O^{\varepsilon 1}$)	–	48.8
*Ser*45 (O^{γ})	*Asp*42 ($O^{\varepsilon 2}$)	–	70.5
*Ser*53 (Oγ)	*Asp*51 ($O^{\delta 1}$)	55.5	4.4
*Lys*54 (*N*)	*Asp*51 ($O^{\delta 2}$)	65.2	6.1
*Glu*59 (*N*)	*Glu*59 ($O^{\varepsilon 1}$)	–	57.3
*Glu*59 (*N*)	*Glu*59 ($O^{\varepsilon 2}$)	–	64.6
*Glu*60 (*N*)	*Glu*60 ($O^{\varepsilon 1}$)	79.5	78.1
*Glu*60 (*N*)	*Glu*60 ($O^{\varepsilon 2}$)	60.0	41.6
*Asn*64 (*N*)	*Glu*68 ($O^{\varepsilon 1}$)	94.0	41.0
*Asn*64 ($N^{\delta 2}$)	*Glu*68 ($O^{\varepsilon 1}$)	51.2	41.0
*Ala*65 (*N*)	*Glu*68 ($O^{\varepsilon 2}$)	97.8	77.2
*Ser*75 (O^{γ})	*Tyr*80 (O^{η})	–	59.4
*Asn*76 ($N^{\delta 2}$)	*Ser*48 (*O*)	–	35.1
*Asn*76 ($N^{\delta 2}$)	*Tyr*80 (O^{η})	49.9	93.6

Table 2 (*Continued*)

Residue		Permanence time (%)	
Donor	Acceptor	H_2O[a]	D_2O[b]
*Lys*77 (N^{η})	*Asn*99 (O^{2})	–	29.6
*Ser*81 (N)	*Ser*45 (O^{γ})	92.8	11.2
*Gln*88 ($N^{\varepsilon 2}$)	*Ser*85 (O)	–	30.4
*Gly*89 (N)	*Gln*88 ($O^{\varepsilon 1}$)	–	35.2
*Lys*95 (N^{η})	*Glu*79 ($O^{\varepsilon 1}$)	–	32.0
*Thr*97 ($O^{\gamma 1}$)	*Glu*79 ($O^{\varepsilon 2}$)	82.6	81.3
*Asn*99 ($N^{\delta 2}$)	*Gly*78 (O)	47.1	–
*Asn*99 ($N^{\delta 2}$)	*Glu*79 ($O^{\varepsilon 1}$)	58.5	–
*Asn*99 ($N^{\delta 2}$)	*Glu*79 ($O^{\varepsilon 2}$)	40.0	–
*Asn*99 ($N^{\delta 2}$)	*Ser*20 (O^{γ})	–	33.9
*Asn*99 ($N^{\delta 2}$)	*Asn*99 (O^{1})	–	36.8

[a] Data from Ciocchetti et al. [24].
[b] MD data are obtained by averaging results from the time interval 100–1100 ps.

able to the increased strength of the solvent–solvent bonding in D_2O [12,17]. This hypothesis is supported by some recent simulation and experimental studies. Schiffer et al. [42] have shown, by MD on a DNA binding domain of the 434 repressor, an increase in the H-bonds number and percentage in correspondence of either a strengthening of the solvent–solvent interaction or a weakening of the protein–solvent interaction. A similar result has been also found in two other MD simulations when H_2O is substituted with more hydrophobic solvents such as methyl hexanoate [23] and chloroform [22]. In addition, Norin et al. [23] suggest that a hydrophobic solvent favors closer contacts among protein polar atoms leading to a diminished solvent exposure of charged and hydrophilic residues. Finally, the H/D isotope effects, experimentally observed on the dynamics of a protein folding reaction, have been also interpreted in terms of an enhancement of the hydrophobic interaction which is favored from a stronger solvent–solvent hydrogen bond in D_2O [17].

The higher degree of the intramolecular hydrogen bonding registered in D_2O may play some role in the higher thermostability of proteins experimentally observed in heavy water [16,10]. On the other hand, this could also affect the protein large scale motions, which are considered crucial for the activation of the biological functionality.

In this respect, a study of the correlated intramolecular motions may give further insight into the elucidation of the complex mechanism governing the protein functionality. Information on how segments of the structure move relatively to one another can be derived from a dynamical cross-correlation map [24,31,43]. The correlation coefficients of PC atoms in D_2O, averaged over 1000 ps and with an absolute value greater than 0.30, are shown in Fig. 5. The dots in the upper left triangle correspond to motions in the same direction and are represented by positive values, whereas in the lower right triangle are shown the negative values, indicative of motions in opposite directions. The data presented in Fig. 5 suggest that proximal residues tend to have positive correlation coefficients, denoted by the broadening of the diagonal in the upper right-hand corner. However, several dots and clusters, indicative of correlated motions occurring among distant residues, are also present.

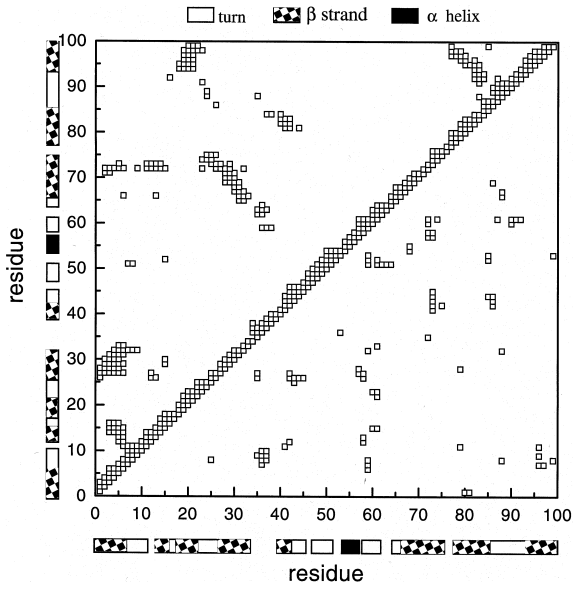

Fig. 5. Dynamical cross-correlation map, $C_{ij} = (\langle r_i r_j \rangle - \langle r_i \rangle - \langle r_j \rangle)\ [(\langle r_i^2 \rangle - \langle r_i \rangle^2)(\langle r_j^2 \rangle - \langle r_j \rangle^2)]^{-1/2}$ for the C_α atom pairs of copper PC using time averaging period of (100–1100) ps. Positive correlations are in the upper left triangle, negative correlations in the lower right triangle. Only correlation coefficients with an absolute value greater than 0.3 are displayed. Secondary elements are also indicated.

The extended clusters refer to positively correlated motions between pairs of β-strands adjacent in the tertiary structure. The coupling of the β-strands is strengthened by the presence of a certain number of H-bonds, which favor the correlated motions between the involved residues. These results witness the importance of the H-bond pattern for concerted motions which, on the other hand, prevent the breakdown of secondary structure elements in the protein. The region of negative correlations shows isolated dots, which mainly correspond to residues located far apart in the tertiary structure of the protein. The comparison of the present data with those previously obtained in H_2O [24], reveals that in both solvents positively correlated motions are centered around the same positions; however, in D_2O the clusters involve a higher number of residues. This effect is particularly evident around positions (Ser20, Ala90) and (Leu5, Lys30). The first cluster refers to correlations between two β strands (1B and 2B) belonging to the same sheet. The second one shows the correlation between the adjacent β strands 2A and 3A. Moreover, the formation of new clusters is observed around positions (Leu5, Phe70) and (Leu12, Phe70). It is interesting to note that these additional correlations are found to correspond to those residues involved in newly formed H-bonds. This result suggests that, besides the stabilization of the tertiary structure, the H-bond interactions play a role in driving the collective motions of the protein, that in D_2O involve a higher number of residues.

Protein dynamics is strictly coupled to the solvent H-bonds network structure and dynamics [44,45]. Details on the spatial and temporal organization of the solvent molecules at the interfacial region can be obtained from two relevant parameters: the average number of H-bonds that each residue forms with the D_2O molecules, $\langle N_{HB} \rangle$, and the average lifetime of the corresponding H-bond [46]. These two quantities are given by:

$$\langle N_{HB} \rangle = N_{HB}/N_{\text{step}} \tag{2}$$

Table 3
$\langle N_{HB} \rangle$, τ, and N_s values averaged over the residue type. The number in parentheses in the first column represents the abundance of each aminoacid residue present in the plastocyanin molecule

Residue type	N_{HB}		τ		N_s	
	H_2O	D_2O	H_2O	D_2O	H_2O	D_2O
Lys[a] (6)	5.27	5.09	21.72	8.52	1434.17	792.00
Asp[a] (7)	9.29	9.38	14.57	15.62	610.14	562.14
Glu[a] (8)	9.10	9.24	15.21	16.34	586.00	466.50
Asn[b] (6)	4.12	3.57	11.56	10.39	483.67	350.67
Gln[b] (1)	5.24	4.52	7.73	5.40	961.00	627.00
His[b] (2)	1.57	0.83	4.66	8.47	187.00	69.50
Tyr[b] (2)	1.97	1.65	13.17	9.43	191.50	137.00
Ser[b] (12)	3.46	3.33	12.38	11.47	526.67	357.00
Thr[b] (2)	3.59	2.93	14.40	14.33	443.50	273.00
Cys[b] (1)	–	–	–	–	–	–
Gly[c] (10)	1.06	1.14	7.52	9.14	162.40	148.00
Ala[c] (7)	1.07	0.87	12.15	16.30	143.00	41.23
Met[c] (2)	0.03	0.04	0.84	8.74	19.00	10.00
Pro[c] (5)	0.82	0.75	10.55	21.28	97.80	52.40
Phe[c] (7)	0.75	0.87	18.93	9.58	93.28	81.28
Leu[c] (6)	0.81	1.52	9.73	8.99	85.50	65.33
Val[c] (9)	0.48	0.54	11.79	7.94	37.00	43.44
Ile[c] (6)	1.05	0.90	19.52	16.14	119.30	76.50

[a] Charged.
[b] Polar.
[c] Polar.

and

$$\tau = \frac{\langle N_{HB} \rangle}{N_s} t_{MD} \quad (3)$$

where, N_{HB} is the total number of H-bonds that are found during the analyzed simulation time, $t_{MD} = 1000$ ps, N_{step} is the number of trajectory frames which is equal to 10^4 and N_s is the number of different solvent molecules engaged in the H-bonds with each residue during the time t_{MD}.

Table 3 shows the $\langle N_{HB} \rangle$, τ and N_s values obtained in the two simulations and averaged over the residue type. The data reflect the dependence of these quantities on the presence of functional groups with different chemico-physical properties which, therefore, induce a different solvent H-bond dynamics near charged, hydrophilic and hydrophobic residues. In this respect, it can be observed that charged residues are able to form a large number of H-bonds. The comparison of the $\langle N_{HB} \rangle$ values formed in H_2O and D_2O, suggests that the capability of H-bond formation is reduced in D_2O for positively charged residues; the opposite behavior appearing to occur for negatively charged residues. The isotopic solvent also reduces the $\langle N_{HB} \rangle$ values on polar residues.

The $\langle N_{HB} \rangle$ value can be, tentatively, connected with the solvent accessible surface area. The reduction of $\langle N_{HB} \rangle$ registered for positively charged and polar residues in heavy water suggests that these residues reduce their exposure to the solvent, by favoring the internal contacts as also evidenced by the increase of the intraprotein H-bonds. This result is in agreement with MD simulation on lipase [23] and BPTI [22]. In our case, the reduction of $\langle N_{HB} \rangle$ for the Lys residues is counter-balanced from the formation of new intramolecular H-bonds (Table 2). In other words, it seems that residues having high ability to form H-bonds that do not match the interaction with the solvent try to find a partner within the protein atoms. Finally, a not well defined trend is observed for hydrophobic residues; such a behavior, could be related to the fact that, in general, only a percentage between 60 and 79% of the hydrophobic surface of a protein is shielded from the solvent [47].

The analysis of τ provides additional information on the dynamics of restructuring of the H-bond network between protein and the two solvents (Table 3). From the comparison of the data obtained in the two simulations it seems that the solvent dependence of τ follows essentially the same trend of $\langle N_{HB} \rangle$. As concerns the charged and the hydrophilic residues, the more remarkable difference between the two solvents is found for Lys and His-like residues. The high average value registered for Lys-like residues in H_2O is mainly due to Lys95, which contributes a τ value of 94.34 ps. The opposite trend is found for His-like residues where a significant increase of τ is registered in D_2O. This result suggests some differences in the dynamical restructuring of the H-bond network in the two solvents.

Since N_s directly reflects the exchange of solvent molecules involved in the protein–solvent H-bond network at the interface, it can be considered as a good reporter of the dynamical behavior of solvent molecules at the interface. In general, the occurrence of high N_s values provides a clear evidence of a rapid exchange of the solvent molecules in the formation of the H-bonds. The data listed in Table 3 show that, although for both solvents a monotonic decrease of N_s is observed going from charged to hydrophobic residues, the frequency of exchange in D_2O is reduced to approximately 30% with respect to H_2O. This strong reduction can probably be traced back to the lower value of the diffusion coefficient of D_2O (0.18 Å^2/ps) compared to that of H_2O (0.23 Å^2/ps). In this respect, it could be hypothesized that the reduced interaction between protein and D_2O molecules could enable higher fluctuations of structural elements involved in the electron transfer pathway (see RMSF results). Fluctuations which are instead functionally regulated by peculiar dynamics of H-bond protein–water network [44]. To assess to whether the different solvent dynamics also correspond to a different solvent organization at the protein–solvent interface, further investigations are required.

4. Conclusion

The analysis of RMSD and RMSF of PC in D_2O has shown that during all the simulation run, the protein preserves its globular shape, which is assured by the general stiffness of its β-structure as already observed in H_2O; while the solvent-exposed regions are more influenced by the dynamics of the solvent. However, a detailed analysis of RMSF has revealed that the structural elements which are supposed to be involved in the electron transfer process show higher RMSF values in D_2O than in H_2O. On the other hand, a result of some interest, also in connection with the possible biological implication, is the increase of the number of the intraprotein H-bonds. In particular, by looking at the functional regions, the hydrophobic patch is more involved in the formation of new H-bonds compared to the hydrophilic patch. This is connected also with an increase of the number of residues involved in concerted motions within the protein molecule, as revealed by the dynamical cross-correlation map. The analysis of protein–solvent H-bond pattern has put into evidence that for all protein residues the frequency of exchange of the solvent molecules involved in the H-bonds with the protein is significantly depressed in D_2O. In this connection, it could be hypothesized that the D_2O dynamics at the protein surface could allow higher fluctuations of protein regions likely involved in the electron transfer pathway, which are instead kept rigid in H_2O. This could be consistent with the fact that in D_2O the protein intramolecular interactions successfully compete with those involving the solvent which are instead more favored in H_2O. Such a fact, which in PC determines a close packing of the protein atoms, may be responsible for the higher protein thermostability in D_2O.

References

[1] R.B. Gregory, M. Dekker, Inc, New York-Basel-Hong Kong, 1995.
[2] J.A. Rupley, G. Careri, Adv. Prot. Chem. 4 (1991) 37.
[3] S.J. Prestrelski, N. Tedeschi, T. Arakawa, J.F. Carpenter, Biophys. J. 65 (1993) 661.
[4] A.R. Bizzarri, S. Cannistraro, Phys. Rev. E 53 (1996) 3040.
[5] A.R. Bizzarri, C. Rocchi, S. Cannistraro, Chem. Phys. Lett. 263 (1996) 559.
[6] R. Abseher, H. Schreiber, O. Steinhauser, Proteins. Struct. Funct. Genet. 25 (1996) 366.
[7] A.R. Bizzarri, S. Cannistraro, Eur. Phys. Lett. 37 (1997) 201.
[8] K. Gekko, S.N. Timasheff, Biochemistry 20 (1981) 4667.
[9] R. Guzzi, L. Sportelli, App. Magn. Res. 9 (1995) 217.
[10] R. Guzzi, L. Sportelli, C. La Rosa, D. Milardi, D. Grasso, J. Phys. Chem. B 102 (1998) 1021.
[11] G. Nemethy, H.A. Scheraga, J. Chem. Phys. 41 (1964) 680.
[12] A. Ben-Naim, J. Will, M. Yacobi, J. Phys. Chem. 77 (1973) 95.
[13] J.S. Finer-More, A.A. Kossiakoff, J.H. Hurley, T. Earnest, Proteins. Struct. Funct. Genet. 12 (1992) 203.
[14] A.A. Kossiakoff, M.D. Sintchak, J. Shpungin, L.G. Presta, Proteins Struct. Funct. Genet. 12 (1992) 223.
[15] V. Lounnas, B.M. Pettitt, Proteins Struct. Funct. Genet. 18 (1994) 133.
[16] G.I. Makhatadze, G.M. Clore, A.M. Gronenburn, Nat. Struct. Biol. 2 (1995) 852.
[17] M.J. Parker, A.R. Clarke, Biochemistry 36 (1997) 5786.
[18] M. Levitt, R. Sharon, Proc. Natl. Acad. Sci. USA 85 (1988) 7557–7561.
[19] P.J. Steinbach, R.J. Loncharich, B.R. Brooks, Chem. Phys. 158 (1991) 383.
[20] V. Lounnas, B.M. Pettitt, G.N. Phillips, Jr., Biophys. J. 66 (1994) 601.
[21] V.A. Makarov, M. Feig, B.K. Andrews, B.M. Pettitt, Biophys. J. 75 (1998) 150.
[22] D.S. Hartsough, K.M. Merz, Jr., J. Am. Chem. Soc. 115 (1993) 6529.
[23] M. Norin, F. Haeffner, K. Hult, O. Edholm, Biophys. J. 67 (1994) 548.
[24] A. Ciocchetti, A.R. Bizzarri, S. Cannistraro, Biophys. Chem. 69 (1997) 185.
[25] W.F. van Gunsteren, H.J.C. Berendsen, Groningen Molecular Simulation (GROMOS) Library Manual, Biomos, Groningen, 1987.
[26] J.M. Guss, H.C. Freeman, J. Mol. Biol. 169 (1983) 521.
[27] M.R. Redinbo, T.O. Yeates, S. Merchant, J. Bioenergy Biomembr. 26 (1994) 49.
[28] C.X. Wang, A.R. Bizzarri, Y.W. Xu, S. Cannistraro, Chem. Phys. 183 (1994) 155.
[29] J.P. Ryckaert, G. Ciccotti, H.J.C. Berendsen, J. Comput. Phys. 23 (1977) 327.
[30] V. Daggett, M. Levitt, Annu. Rev. Biophys. Biomol. Struct. 22 (1993) 353.
[31] P.H. Hunenberger, A.E Mark, W.F. van Gunsteren, J. Mol. Biol. 252 (1995) 492.
[32] J.M. Guss, H.D. Bartunik, H.C. Freeman, Acta Cryst. B48 (1992) 790.
[33] S. Young, K. Sigfridsson, K. Olesen, O. Hansson, Biochim. Biophys. Acta 1322 (1997) 106.

[34] R. Langen, I.J. Chang, J.P. Germanas, J.H. Richards, J.R. Winkler, H.B. Gray, Science 268 (1995) 1733.
[35] K.W. Penfield, A.A. Gewirth, E.I. Solomon, J. Am. Chem. Soc. 107 (1988) 4519.
[36] E.I. Solomon, M.J. Baldwin, M.D. Lowery, Chem. Rev. 92 (1992) 521.
[37] C. Rocchi, A.R. Bizzarri, S. Cannistraro, Chem. Phys. 214 (1997) 261.
[38] C. Rocchi, A.R. Bizzarri, S. Cannistraro, Phys. Rev. E 57 (1998) 3515.
[39] J.A. McCammon, S.C. Harvey, Dynamics of Proteins and Nucleic Acids, Cambridge University Press, Cambridge, 1987.
[40] D.L. Smith, Y. Deng, Z. Zhang, J. Mass. Spectrom. 32 (1997) 135.
[41] P.J.F. de Rege, S. Williams, M.J. Therien, Science 269 (1993) 1409.
[42] A. Schiffer, V. Dotsch, K. Wuthrich, W.F. van Gunsteren, Biochemistry 34 (1995) 15057.
[43] W.E. Harte, S. Swaminathan, M.M. Mansuri, J.C. Martin, I.E. Rosenberg, D.L. Beveridge, Proc. Natl. Acad. Sci. USA 87 (1990) 8864.
[44] W. Doster, A. Bachleitner, R. Dunau, M. Hiebl, E. Luscher, Biophys. J. 50 (1986) 213.
[45] C. Arcangeli, A.R. Bizzarri, S. Cannistraro, Chem. Phys. Lett. 291 (1998) 7.
[46] A.R. Bizzarri, C.X. Wang, W.Z. Chen, S. Cannistraro, Chem. Phys. 201 (1995) 463.
[47] K.P. Murphy, S.J. Gill, J. Mol. Biol. 222 (1991) 699.